Identification of the Molecular Targets of Disulfide Bond Disrupting Agents

[1]Mary E. Law, [2]Elham Yaaghubi, [2]Amanda F. Ghilardi, [1]Bradley J. Davis, [2]Renan B. Ferreira, [3]Jin Koh, [3,4]Sixue Chen, [2]Sadie F. DePeter, [2]Christopher M. Schilson, [5]Chi-Wu Chiang, [6,7]Coy D. Heldermon, [8]Peter Nørgaard, [2,7]Ronald K. Castellano[#], and [1,7]Brian K. Law[#]

Affiliations

[1]Department of Pharmacology & Therapeutics, University of Florida, Gainesville, FL 32610 USA.

[2]Department of Chemistry, University of Florida, Gainesville, FL 32611 USA.

[3]Proteomics and Mass Spectrometry Facility, Interdisciplinary Center for Biotechnology Research, University of Florida, Gainesville, FL 32610 USA.

[4]Department of Biology, Genetics Institute, University of Florida, Gainesville, FL 32610 USA

[5]Institute of Molecular Medicine, College of Medicine and Center for Infectious Disease and Signaling Research, National Cheng Kung University, Tainan, Taiwan.

[6]Department of Medicine, University of Florida, Gainesville, FL 32610 USA.

[7]UF-Health Cancer Center, University of Florida, Gainesville, FL 32610 USA.

[8]Department of Pathology, Copenhagen University Hospital Herlev, DK-2730 Herlev, Denmark.

[#]Co-Contributing Corresponding Authors

Running Title: Molecular Targets of DDAs

Abstract

Breast cancer mortality remains unacceptably high, indicating a need for safer and more effective therapeutic agents. Disulfide bond Disrupting Agents (DDAs) were previously identified as a novel class of anticancer compounds that selectively kill cancers that overexpress the Epidermal Growth Factor Receptor (EGFR) or its family member HER2. DDAs kill EGFR+ and HER2+ cancer cells via the parallel downregulation of EGFR, HER2, and HER3 and activation/oligomerization of Death Receptors 4 and 5 (DR4/5). However, the mechanisms by which DDAs mediate these effects are unknown. Affinity purification analyses employing biotinylated-DDAs reveal that the Protein Disulfide Isomerase (PDI) family members AGR2, AGR3, PDIA1, and ERp44 are DDA target proteins. Further analyses demonstrate that shRNA-mediated knockdown of AGR2 and ERp44, or expression of ERp44 mutants, enhance basal and DDA-induced DR5 oligomerization. DDA treatment of breast cancer cells disrupts PDIA1 and ERp44 mixed disulfide bonds with their client proteins. Together, these results reveal DDAs as the first small molecule, active site inhibitors of AGR2 and ERp44, demonstrate a role for AGR2 and ERp44 in regulating the activity, stability, and localization of DR4 and DR5, and nominate ERp44 as a new molecular target for anticancer therapeutics.

Key Words: Apoptosis, Cancer, Disulfide bond Disrupting Agents, DR5, DR4, EGFR, AGR2, ERp44, PDIA1

Introduction

In spite of significant improvements in early detection, and multiple new molecularly targeted therapeutics, breast cancer remains the second largest cancer killer of women in America after lung cancer, and is the most frequently diagnosed cancer in American women [1]. Much of the lethality of breast cancer derives from our inability to successfully treat patients with metastatic and/or drug-resistant malignancies. New drugs are needed that bypass resistance to currently used regimens by targeting cancer cell-specific vulnerabilities. A class of agents termed Disulfide bond Disrupting Agents (DDAs) was previously identified and shown to kill breast cancer cells in association with downregulation of the HER-family proteins EGFR, HER2, and HER3, and decreased activating phosphorylation of the Akt kinase [2]. Subsequent work showed that DDAs induce endoplasmic reticulum stress (ERS) [3] and alter the pattern of disulfide bonding of EGFR and the TRAIL receptors, Death Receptor 4 (DR4) and Death Receptor 5 (DR5) [4]. DDA-induced cell death is mediated by activation of the Caspase 8-Caspase 3 extrinsic apoptotic pathway.

Little is known regarding how the disulfide bonding of HER-family and Death Receptor-family proteins are facilitated within the endoplasmic reticulum, and how the disulfide bonding patterns of these proteins control their stability, intracellular localization, and downstream signaling. TNF-Related Apoptosis Inducing Ligand (TRAIL) has been considered a promising cancer therapeutic agent due to its selectivity for killing cancer cells, while leaving normal tissues unharmed [5-8]. However, TRAIL analogs and DR4/5 agonistic antibodies have yet to be clinically approved for anticancer therapy. This is due in part to pharmacokinetic issues related to these protein drugs themselves, and in part to the ability of cancer cells to acquire resistance by downregulating DR4 and DR5 (reviewed in [9]). Since DDAs upregulate DR5 and activate DR4 and DR5 in a ligand-independent manner [4, 10], DDAs may overcome the resistance mechanisms that suppress the efficacy of other activators of the TRAIL/Death Receptor pathway. A recent report showed that the extracellular domain of DR5 prevents oligomerization and downstream activation of Caspase 8 in the absence of ligand

engagement, and that excision of the DR5 extracellular domain permits full activation of DR5 in a ligand-independent manner [11]. It was previously proposed that DDAs activate DR5 in a ligand-independent manner by permitting inter-molecular disulfide bond formation at the expense of intramolecular disulfide bonding, resulting in DR5 oligomerization and activation [4, 10]. However, the precise mechanisms through which this happens are unknown. Similarly, DDA treatment causes disulfide bond-dependent EGFR oligomerization followed by degradation [2, 4], but how DDAs perturb EGFR disulfide bonding is unknown. The Protein Disulfide Isomerase (PDI) family member AGR2 is essential for EGFR folding and surface localization [12], and likewise facilitates expression of Mucins [13, 14].

The PDI family contains 21 members (reviewed in [15]). Although significant attention has focused on the roles of canonical PDIs in mediating disulfide bond formation via their active site thioredoxin-like CXXC motifs, and canonical PDIs are considered promising targets for anticancer therapeutics [16], the other PDI family members are less well studied. The PDI proteins AGR2 and AGR3 contain a non-canonical CXXS active site motif. Based on biochemical PDI mutagenesis studies [17] it is predicted that AGR2/3 will exhibit disulfide isomerase activity, but not oxidase or reductase activity. Consistent with this, AGR2 forms stable mixed disulfide bonds with its client proteins [12, 13]. Another PDI family member, ERp44, also contains an active site CXXS motif, and has multiple functions within the endoplasmic reticulum (ER). ERp44 plays a critical role in the disulfide-mediated oligomerization of Adiponectin [18, 19] and Immunoglobulin M [20, 21]. Additionally, ERp44 anchors client/partner proteins such as ERO1α, Prx4, FGE/SUMF1, and ERAP1 [22-25] that do not contain their own C-terminal -KDEL ER retention sequences to prevent their secretion (reviewed in [26]).

HER-family proteins are the only sub-family of receptor tyrosine kinases that contain two cysteine-rich repeats in their extracellular domain [27]. DR4 and DR5 also harbor numerous disulfide bonds in their extracellular domains [28]. Based on these observations, we previously hypothesized

that HER-family proteins and DR4/5 may be particularly sensitive to agents that impede native disulfide bond formation. Despite the thiol-reactivity of DDAs [2], the mechanisms by which they cause downregulation of EGFR, HER2, HER3 and activation of DR4/5 are unknown. Here we show using novel biotinylated DDA derivatives that DDAs covalently modify AGR2, PDIA1, and ERp44 in vitro and in intact cells, and that DDA treatment of cells disrupts PDIA1 and ERp44 disulfide bonds with their client proteins. Together, the results indicate that DDAs activate DR4/5 and inactivate EGFR, HER2, and HER3 by inhibiting the activity of the PDI family members AGR2, PDIA1, and ERp44, which mediate native disulfide bonding of these transmembrane receptors. DDAs are the first agents to our knowledge that function in part by modifying the active site Cys residues of AGR2 and ERp44.

Results

Characterization of novel DDAs with enhanced potency: Previously described DDAs, including RBF3, DTDO, and tcyDTDO (Fig. 1A), were demonstrated to suppress tumor growth through induction of apoptotic cancer cell death [4, 29]. However, whether DDAs exhibit anticancer activity when administered orally, or if they have efficacy against liver metastases, was not examined. The HCI-001/LVM2 model was obtained from the HCI-001 Patient-Derived Xenograft [30] by two rounds of selection for liver metastasis [4]. Mice bearing HCI-001/LVM2 breast tumors were treated once daily for four consecutive days with 20 mg/kg tcyDTDO by oral gavage and livers were collected. Liver metastases in the tcyDTDO treated animals exhibited central necrosis (Fig. 1B, yellow arrows). Although central necrosis can occur in tumors due to an insufficient blood supply, necrosis is not observed in vehicle treated tumors, indicating that the tumor cell death is caused by tcyDTDO treatment.

As revealed from our previous studies, modifications of the parent cyclic DDA, DTDO, resulted in a more potent DDA, tcyDTDO, with improved pharmacodynamic and pharmacokinetic properties [4, 10, 29]. With tcyDTDO in hand, we then explored the effect of substitutions on its cyclohexane ring to determine if its potency and drug-like properties could be further improved. Our efforts led to the design and synthesis of novel DDAs including dimethoxy-tcyDTDO (dMtcyDTDO) and difluoro-tcyDTDO (dFtcyDTDO) (Fig. 1C). Well appreciated, fluorine's size and high electronegativity lead to strong C–F bonds that resist metabolic degradation making fluorine substitution an effective way to increase drug stability. For instance, it has been shown that replacing hydrogen with fluorine significantly alters the rate and extent of Cytochrome P450 metabolism [31-34]. Both dMtcyDTDO and dFtcyDTDO exhibit approximately two-fold greater potency than tcyDTDO in cell viability assays (Fig. 1D). DMtcyDTDO also exhibited two-fold greater potency than tcyDTDO in DNA and protein synthesis assays (Fig. S1A). DDAs were previously shown to induce apoptotic cell death associated with ERS, disulfide bond-mediated oligomerization of Death Receptors 4 and 5 (DR4/5) and EGFR,

and upregulation of DR5 [2-4, 29]. Therefore, we examined the effect of the novel DDAs on disulfide bonding of these proteins by immunoblot analysis under non-reducing conditions ([4] and Supplemental Information). When applied to cancer cells at the same concentration, dMtcyDTDO and dFtcyDTDO induced more DR4/5 oligomerization, higher DR5 levels, and produced greater ERS (Fig. 1E, left panel). Induction of ERS by dFtcyDTDO and dMtcyDTDO, as indicated by GRP78 elevation, and disulfide-mediated oligomerization of DR4 and EGFR, was detected at 625 nM and oligomerization of DR5 was observed at 1.25 μM of each compound (Fig. 1E, right panel). Additional immunoblot analyses performed under reducing conditions revealed that dMtcyDTDO is more potent than tcyDTDO in the induction of HER3 downregulation, DR5 upregulation, and ERS as indicated by elevated CHOP and XBP1s (Fig. S1B). Time-course and concentration-response analyses of these endpoints showed that dMtcyDTDO induced these responses as early as four hours after treatment (Fig. S1C).

Tumor studies using the HER2+ BT474 xenograft model [2] were performed to examine if dMtcyDTDO and dFtcyDTDO induce rapid breast cancer cell death as observed with tcyDTDO. Tumors from animals treated with the vehicle for four consecutive days did not show evidence of tumor necrosis (Fig. 1F). In contrast, tumors were not observed in mammary fat pads from dFtcyDTDO treated animals. Mammary glands from dMtcyDTDO treated animals exhibited tumors that had undergone coagulation necrosis, consistent with rapid and uniform death of the cancer cells.

AGR2 as a DDA binding protein: To understand how DDAs kill breast tumors, knowledge of their direct protein targets is essential. The development of molecular probes proved crucial in identifying DDA biological targets and linking them to the observed DDA responses. Furthermore, knowledge of the DDA binding site enables rational design of optimized next-generation DDAs. For this purpose, we used activity-based protein profiling and standard affinity pulldown techniques with biotin as the affinity label.

To generate DDA probes, we sought a biologically active cyclic DDA with a functional group that enables installation of a biotin tag. This was achieved by fusing a Boc-protected pyrrolidine ring at the 4,5-positions of the parent DTDO compound to generate (±)-BocPyrDTDO (Fig. 2A), which is biologically active and showed a potency similar to DTDO (Fig. S1D). The synthesis of (±)-BocPyrDTDO was accomplished by cleaving the acetyl groups of dithioacetate (±)-**3** followed by oxidation to furnish the 1,2-dithiane 1,1-dioxide ring (Fig. 2A). Intermediate (±)-**3** can be obtained through a few functional group interconversion steps from diester (±)-**1** which itself could be obtained according to literature procedures. The amino group on the pyrrolidine ring, after Boc group deprotection, enables installation of the linker and biotin tag as described in full detail in the Supplementary Information. Biotinylated DDA analogs, including Biotin-PyrDTDO (BPD) and Biotin-GlyPyrDTDO (BGPD), were generated in this fashion and used as affinity tags to identify DDA targets (Fig. 2A).

The protein disulfide isomerase (PDI) family member AGR2 was previously implicated in disulfide bonding of EGFR [12], and DDAs alter EGFR disulfide bonding ([4] and Fig. 1E, right panel). We hypothesized that AGR2 might be a target of DDAs and examined if biotinylated DDAs bind covalently with recombinant AGR2. Biotin-GlyPyrDTDO labeled AGR2 in a concentration-dependent manner (Fig. 2B). We further hypothesized that in addition to EGFR, DR4 or DR5 may be AGR2 client proteins. Stable knockdown of AGR2 in breast cancer cells increased disulfide-mediated DR5 oligomerization and increased Caspase 8 cleavage/activation (Fig. 2C, CC8). AGR2 forms mixed disulfide bonds to its client proteins with Cys81 in its thioredoxin-like repeat [13], and Cys81 is the only Cys residue present in AGR2. Therefore, we examined if mutating Cys81 to Serine prevented DDA labeling. The C81S AGR2 mutant was not labeled by Biotin-GlyPyrDTDO (Fig. 2D). AGR3 is the PDI paralog most closely related to AGR2 and it was also labeled by Biotin-GlyPyrDTDO. Addition of a molar excess of dMtcyDTDO to the labeling reactions partially prevented Biotin-GlyPyrDTDO binding to AGR2 and AGR3 (Fig. 2D), suggesting competition for binding to the same Cys residue(s).

A comparison of the ability of dMtcyDTDO and tcyDTDO to block Biotin-GlyPyrDTDO binding to AGR2 indicated that dMtcyDTDO was a more effective competitor, suggesting that competition in this binding assay reflects DDA potency (Fig. 2E, S1E, F).

Identification of PDIA1 and ERp44 as DDA target proteins: A panel of three breast cancer cell lines was treated with Biotin-PyrDTDO to label DDA target proteins in intact cells. Two biotinylated proteins that were observed exclusively in the context of cell labeling with Biotin-PyrDTDO were termed DDA target proteins 1 and 2 (DDAT1/2). DDAT1/2 migrated at 60 kDa and 44 kDa, respectively, and were observed in three different breast cancer lines in crude cell extracts and in samples purified using Streptavidin-agarose (Fig. 3A). The Streptavidin-agarose purification was scaled up to generate DDAT1/2 in sufficient amounts for identification by mass spectrometry, and small amounts of this preparation and the corresponding crude extracts were analyzed by blotting with Streptavidin-Alkaline Phosphatase, and by silver staining (Fig. 3B). DDAT1 and DDAT2 from a Coomassie stained gel were excised and analyzed by trypsin digestion followed by mass spectrometry as described in Materials and Methods. DDAT1 and DDAT2 were identified as the PDI-family members ERp44 and PDIA1, respectively (Fig. S2A, S2B). In support of these assignments, ERp44, PDIA1, and AGR2 were isolated from the luminal A T47D and luminal B BT474 breast cancer cell lines treated with Biotin-PyrDTDO using Streptavidin-Agarose (Fig. 3C, left panel). In additional Biotin-PyrDTDO pulldown experiments, ERp44 and PDIA1 were detected, but the PDIs ERp57 and ERp5 were not (Fig. S2C). Endogenous proteins are biotinylated via amide linkages. Thus, DDAT1 and DDAT2 are distinguished from endogenous biotinylated proteins by disruption of Biotin-DDA/target protein linkages with the reducing agent 2-Mercaptoethanol (Fig. S2D). Immunoprecipitation with an AGR2 antibody showed that ERp44 and PDIA1 co-purify with AGR2 from cells irrespective of treatment with Biotin-PyrDTDO (Fig. 3C, left panel). ERp44 immunoprecipitates contained PDIA1, but AGR2 co-purification was not detected. Biotin-PyrDTDO/Streptavidin-Agarose also affinity purified ERp44 and

PDIA1 from the MDA-MB-468 Triple-Negative breast cancer cell line (Fig. 3C, right panel). In vitro binding studies showed that Biotin-PyrDTDO labeled ERp44 and PDIA1, and in both cases, biotinylation was blocked by pre-incubation with a molar excess of dMtcyDTDO (Fig. 3D). If ERp44 and PDIA1 are cellular DDA targets, then DDA treatment may alter the pattern of ERp44 and PDIA1 disulfide bonding with their client proteins. Consistent with this, treatment of breast cancer cells with dMtcyDTDO reduces disulfide bonding of ERp44 and PDIA1 with multiple proteins (Fig. 3E, red arrows) with minimal effect on monomeric levels of ERp44 and PDIA1. PDIA1 is a validated target for anticancer drugs [16]. However, ERp44 has not been investigated extensively as a therapeutic target for cancer, and small molecule ERp44 inhibitors have not been reported. Similarly, small molecule AGR2 inhibitors have not been reported. Therefore we focused most of our efforts on characterizing AGR2 and ERp44 as DDA target proteins.

A role for ERp44 in the control of Death Receptor and EGFR disulfide bonding: Immunoblot analysis of a panel of breast cancer cell lines revealed that PDIA1 levels were similar among the lines (Fig. 4A). In contrast, ERp44, AGR2, and AGR3 levels varied among the lines, as did the oxidoreductase ERO1, which plays a key role in producing oxidizing equivalents for disulfide bond formation [16, 35-37]. ERp44 co-immunoprecipitation experiments showed that ERp44 associates with DR5, DR4, ERO1, and AGR2 in MDA-MB-468 cells (Fig. 4B). The interactions are non-covalent because although the analyses were performed under non-reducing conditions, each protein migrated as a monomer. A BT474 cell line stably overexpressing ERp44 was generated to examine the effect of elevated ERp44 levels on DR4/5 disulfide bonding and DDA responses. ERp44 overexpression reduced DDA induction of high molecular mass DR4 oligomers, and to a lesser extent high molecular mass DR5 oligomers (Fig. 4C, left panel, red arrows). In both cases, the overall pattern was a shift from high to lower molecular mass disulfide-bonded species. These oligomeric protein forms were not observed when the analyses were performed under reducing conditions (Fig. 4C, right panel). Next,

ERp44 knockdown MDA-MB-468 cells were generated and the effect on DR4/5 disulfide bonding examined. Although we were only able to achieve modest ERp44 knockdown in multiple independent experiments, ERp44 knockdown consistently increased high molecular mass oligomers of DR4, DR5, and EGFR at the interface between the stacking gel and the resolving gel in the absence of DDA treatment (Fig. 4D, left panel, red arrows; expanded view in Fig. 4D, right panel, red asterisks). ERp44 knockdown increased PDIA1 oligomerization and increased dMtcyDTDO induction of Caspase 8 cleavage/activation (CC8). Together, the results of the AGR2 and ERp44 knockdown experiments are consistent with roles for AGR2 and ERp44 in facilitating native disulfide bond formation of DR4 and DR5, and DDAs blocking these AGR2 and ERp44 functions.

We next examined if mutations within the thioredoxin-like repeat of ERp44 alter DR5 levels and disulfide bonding, and other DDA responses. Overexpressed, wild type ERp44 exhibited a high level of disulfide bond-mediated complex formation with client proteins (Fig. 5A). Both endogenous and overexpressed ERp44 monomers migrated as a doublet. This was previously shown to result from differential O-linked glycosylation [38]. In contrast, the DR5 monomer doublet is caused by alternative splicing. The C58S ERp44 mutant (SXXS), which lacks a Cys residue in its thioredoxin-like repeat, showed lower binding to client proteins, although the levels of the monomer were similar to that of the wild type protein. The S61C ERp44 mutant (CXXC) exhibited slightly increased oligomerization compared with wild type ERp44. We previously showed that DDAs alter the electrophoretic mobility of EGFR and CUB Domain-Containing Protein 1 (CDCP1), block the formation of complexes between these two proteins, and alter their tyrosine phosphorylation patterns [39]. Overexpression of both ERp44 point mutants was associated with increased oligomerization of EGFR and CDCP1, but did not alter the ratio between the full length (FL) and cleaved (Cl.) forms of CDCP1. Overexpressed ERp44 exhibited disulfide bonding to client proteins (e.g., bands marked by asterisks) and these interactions were partially blocked by dFtcyDTDO treatment (Fig. 5B). As observed in Fig. 5A, the C58S mutant showed decreased binding to client proteins. Interestingly, the

S61C ERp44 mutant bound client proteins similarly to the wild type protein, but was less sensitive to disruption of binding to its clients by dFtcyDTDO. ERp44 overexpression had little effect on DR5 levels with or without dFtcyDTDO treatment. In contrast, overexpression of either the C58S or S61C ERp44 mutants modestly increased steady-state DR5 expression and potentiated DR5 upregulation by dFtcyDTDO. Overexpression of ERp44 and its mutants modestly increased PDIA1 levels and binding to its client proteins. Consistent with the C58S ERp44 mutant inducing the strongest potentiation of DR5 upregulation by dFtcyDTDO, expression of this mutant was also associated with partial oligomerization of EGFR in vehicle treated cells that correlated with increased expression of the ERS marker GRP78 (Fig. 5B). Overall, these observations indicate that ERp44^{C58S}, and to a lesser extent, ERp44^{S61C}, interfere with disulfide bond formation of ERp44 clients, resulting in higher baseline ERS and potentiating DDA effects on DR4 and DR5. However, these observations do not explain why cancer cells that overexpress EGFR or HER2 have heightened DDA sensitivity [2, 3]. T47D breast cancer cells express low levels of EGFR, HER2, and HER3. Thus, T47D cells were previously used as a model system to study the effects of EGFR overexpression on DDA responses [2, 3, 40]. Examination of ERp44 and PDIA1 disulfide bonding in control and EGFR overexpressing T47D cells showed that EGFR overexpression resulted in recruitment of ERp44 and PDIA1, and to a lesser extent DR4/5, into disulfide-bonded protein complexes (Fig. 5C). Under these conditions, levels of monomeric ERp44 and PDIA1 are reduced. The monomeric forms of ERp44 and PDIA1 are accessible to facilitate native disulfide bonding of their client proteins. Thus, EGFR may increase DDA sensitivity by reducing the pools of monomeric ERp44 and PDIA1 that DDAs must inactivate in order to interfere with native disulfide bond formation of ERp44 and PDIA1 client proteins.

As mentioned earlier, ERp44 mediates quality control of Adiponectin [18] and Immunoglobulin M [21] maturation by shuttling inappropriately disulfide bonded protein forms from the Golgi back into the ER, while permitting secretion of correctly disulfide bonded proteins. We hypothesized that ERp44 may carry out a similar function to facilitate trafficking and folding of transmembrane proteins that

have disulfide bonds in their extracellular domains. Cell labeling using membrane impermeable, protein-reactive probes is useful for confirming the presence of receptors at the cell surface. Surface biotinylation studies performed on cells after treatment with dMtcyDTDO showed increased cell surface levels of DR4 and DR5, irrespective of whether labeling was performed with amine- or thiol-reactive cell-impermeable biotinylation probes (Fig. 5D). This increased accumulation of DR4/5 at the cell surface is consistent with previous findings that DDAs synergize with the DR4/5 ligand TRAIL to induce cancer cell apoptosis [4].

Discussion

Models for DDA mechanisms of action and compound selectivity: The findings presented here, along with previous reports on the mechanisms of DDA action [2-4, 29], suggest the model in Fig. 6A. DDAs bind to the PDI-family proteins ERp44, PDIA1, AGR2, and AGR3 and alter the disulfide bonding of client proteins. These changes in disulfide bonding are associated with upregulation of DR5, oligomerization of DR4 and DR5, and accumulation of DR4 and DR5 at the cell surface. Oligomerization of DR4 and DR5 activates Caspase 8, which in turn activates Caspase 3 to execute apoptosis. Caspase activation plays a key role in downregulating EGFR and HER2, and decreasing Akt phosphorylation because these DDA responses are largely ablated by a pan-Caspase inhibitor [4]. To our knowledge, DDAs are the first small molecule agents targeting ERp44 and AGR2/3. Further, DDAs are the first experimental anticancer agents identified that activate DR4 and DR5-mediated Caspase 8 activation by inducing disulfide bond-mediated DR4/5 clustering in the absence of their ligand TRAIL. A recent report showed that the extracellular domain of DR5 acts to prevent its oligomerization in the absence of TRAIL [11]. DDAs may overcome this autoinhibition by favoring intermolecular disulfide bonding between DR4/5 extracellular domains over intramolecular disulfide bonding.

Previous reports showed that overexpression of EGFR amplifies multiple DDA responses, including ERS induction, DR5 upregulation, HER1-3 downregulation, and reduction of Akt phosphorylation [2-4]. Discovery of ERp44 and PDIA1 as DDA target proteins led to the observation that EGFR overexpression reduces the levels of monomeric ERp44 and PDIA1 accessible for facilitating native disulfide bonding of client proteins. Since DDAs covalently modify monomeric ERp44 and PDIA1 (Fig. 3), these observations reveal the molecular basis for the synthetic-lethal interaction between EGFR overexpression and DDA-based therapies. Given the importance of EGFR as a potential oncogenic driver in a number of cancers, including glioblastoma [41, 42] and Triple-Negative Breast Cancer [43-45], DDAs may have utility against these malignancies.

Because of the relative structural simplicity of DDA molecules, the mechanisms responsible for their target protein selectivity are of interest. PDIA1 has been investigated as a target for anticancer therapeutics, and PDIA1 inhibitors have established anticancer efficacy in preclinical models [46, 47]. AGR2 contributes to tumor progression by facilitating EGFR disulfide bonding and surface presentation [48]. However, AGR2 may also be secreted and promote tumor angiogenesis [49, 50] and act on cell surface receptors [51]. Monoclonal antibodies designed to block extracellular AGR2 functions are under development [51, 52], but agents that block the essential role of AGR2 in the folding of client proteins are not available.

The canonical thioredoxin-like catalytic site sequence CXXC is featured in PDIA1 and several other PDI enzymes (reviewed in [15]). Interestingly, the DDA targets AGR2, AGR3, and ERp44 share a non-canonical CXXS thioredoxin-like repeat sequence (Fig. 6B). A report employing both yeast genetics and biochemical enzyme assays showed that the essential function of the PDI enzyme for yeast survival is catalysis of disulfide exchange or “scramblase” activity and that this could be carried out by the CXXS mutant of PDI (PDI^{CXXS}) [17]. Enzyme assays showed that PDI^{CXXS} could reactivate inappropriately disulfide bonded RNAse A via its scramblase activity. In contrast, PDI^{CXXS} was unable to catalyze disulfide bond oxidation or reduction like the wild type PDI^{CXXC} enzyme.

The C-terminal Cys residue in the CXXC motif of PDIs accelerates substrate release. Consequently, CXXS substrate-trapping mutants of PDIs have been used to isolate mixed disulfide bonded dimers with their client/substrate proteins [53, 54]. That the CXXS motif is associated with slow client protein off-rate is consistent with the established roles of ERp44 in retaining specific client/partner proteins such as ERO1 [22] and ERAP1 [25] in the ER, and in retrotranslocation of inappropriately disulfide bonded Adiponectin [55, 56] and IgM [21, 57] from the Golgi to the ER. Thus, the CXXS motifs of AGR2, AGR3, and ERp44 bound to DDAs may exhibit a slow off-rate for the same reason.

The DDA pharmacophore has the capacity to adopt cyclic or linear structures (Fig. 1, [2]). Reaction of a protein-associated Cysteine thiolate nucleophile with the electrophilic sulfenyl sulfur atom on the thiosulfonate moiety of cyclic DDAs opens the ring and generates the linear DDA form containing a free nucleophilic sulfinate group that can mount an attack on the disulfide bond to regenerate the cyclic DDA and excise itself from the protein (acting as reversible covalent ring opening/closing inhibitors) (Fig. 6C). Thus, the proteins targeted by DDAs are predicted to be those that stabilize the linear form of the DDAs by appropriate noncovalent interactions to slow the corresponding back reaction (cyclization and auto-excision).

It is clear from the experiments with intact cancer cells that DDAs alter the disulfide bonding of DR4, DR5, and EGFR and change the pattern of disulfide bonding between ERp44 and PDIA1 and their client proteins. It is difficult to compare DDAs actions with those of published inhibitors of PDI activity since these studies often to do not examine perturbation of protein disulfide bonding in cancer cells, but rather examine compound activity in the Insulin reduction/aggregation assay. While the Insulin reduction assay is valuable for optimizing the potency of PDI inhibitors, it may not be salient in instances where disulfide isomerase activity is more important than disulfide oxidase or reductase activity.

In summary, DDA selectivity for killing cancer cells and for stably binding to its target proteins derives from the following combination of factors: 1. EGFR or HER2 overexpression in cancer cells limits the pool of free ERp44 and PDIA1 available to mediate disulfide bonding of clients such as DR4, DR5, and EGFR itself; 2. Some potential DDA targets may have the capacity to excise DDAs using Cysteine residues adjacent to the DDA-modified Cysteine; and 3. DDAs have the ability to auto-excise by cyclization, therefore target proteins must stabilize the linear form of the bound DDA. Interest in covalent protein targeting drugs is increasing because temporal target engagement is less limited by their pharmacokinetic properties than non-covalent therapeutics. DDAs exemplify how covalent drugs may be utilized to kill cancer cells with minimal effects on normal cells. Further, the

observation that tumor sensitivity to DDAs will vary inversely with the levels of monomeric DDA target proteins (e.g., Fig. 5C) may inspire the development of predictive diagnostic tests of tumor biopsies that identify the patients that are most likely to benefit from DDA-based treatment regimens.

Materials and Methods

Cell culture, preparation of cell extracts, and immunoblot analysis

The BT20, BT474, BT549, MCF7, MDA-MB-231, MDA-MB-436, MDA-MB-468, HCC1143, HCC1500, HCC1569, HCC1937, HCC1954, Hs578t, and T47D cells lines were purchased from American Type Culture Collection (ATCC) (Manassas, VA). The HCI-001 cell line was derived from an ER-/PR-/HER2- patient-derived xenograft originally isolated from a patient as described previously [58]. The HCI-001/LVM2 model was derived from the HCI-001 cell line by performing two rounds of selection for liver metastasis, as described previously [4]. Cell lines were grown in Dulbecco's Modified Eagle's Medium (GE Healthcare Life Sciences, Logan, UT) containing 10% fetal bovine serum (10% FBS–DMEM) in a humidified incubator with 5% CO_2 at 37^{o}C. Cell lysates were prepared as described previously [59]. Immunoblot analysis was performed utilizing the following antibodies purchased from Cell Signaling Technology (Beverly, MA) [Akt, #4691; P-Akt[T308], #13038; ATF4, #11815; CHOP, #2895; Cleaved Caspase 8, #9496; DR4, #42533; DR5, #8074; EGFR, #4267; GRP78, #3177; HER3, #4754; PARP, #9532; PDIA1, #3501; XBP1s, #12782], from Santa Cruz Biotechnology (Santa Cruz, CA) [Actin, sc-47778; AGR2/3, sc-376653; AGR3, sc-390940; ERO1-α, sc-100805; and ERp44, sc-393687], or from Rockland Immunochemicals, Inc. (Limerick, PA), Streptavidin-Alkaline Phosphatase conjugated (SA-AP), S000-05.

Construction of vectors and stable cell lines using recombinant retroviruses and lentiviral shRNAs

Total RNA from T47D cells was extracted with TRIzol Reagent (Invitrogen, Waltham, MA) according to the manufacturer's protocol. Total cellular RNA was used to synthesize first-strand cDNA by using the PCR conditions listed: 25□°C for 10□min, 42□°C for 30□min, and 95□°C for 5□min. PCR was subsequently performed using the following ERp44 primers: 5′-TTTTGGATCCCACCATGCATCCTGCCGTCTTCC-3′ and 5′-

TTTTCTCGAGTTAAAGCTCATCTCGATCCCTC-3′. The PCR fragment encoding ERp44 was subsequently digested with BamHI and XhoI and cloned into the 5' BamHI and 3' XhoI sites of the pMXs-IRES-Blasticidin retroviral vector (RTV-016) (Cell Biolabs, Inc., San Diego, CA). The C58S and S61C mutations of Erp44 were performed using QuikChange mutagenesis and the following primers: 5'- CTTTAGTAAATTTTTATGCTGACTGGAGTCGTTTCAGTCAGATGTTG-3' and 5'-CAACATCTGACTGAAACGACTCCAGTCAGCATAAAAATTTACTAAAG-3' and 5'-GACTGGTGTCGTTTCTGTCAGATGTTGCATCCAATTTTTG-3' and 5'-CAAAAATTGGATGCAACATCTGACAGAAACGACACCAGTC-3', respectively. Mutation of ERp44 was verified by sequencing. The retroviral vector encoding EGFR (Plasmid 11011) was purchased from Addgene (Cambridge, MA). Stable cell lines were constructed as described previously [39, 60]. The ERp44 shRNA lentiviral constructs were obtained from the TRC Lentiviral shRNA Libraries from Thermo Scientific. Stable cell lines were constructed from these lentiviral shRNAs according to vendor protocol.

Thymidine Incorporation Assays

Thymidine incorporation assays were performed as described previously [61].

Protein Synthesis Assays

Protein synthesis assays utilizing ^{3}H-Leucine purchased from Perkin Elmer (Waltham, MA) were carried out as detailed previously [62, 63].

Cell viability assays

MTT (3-(4,5-dimethylthiazol-2-yl)-2,5-diphenyltetrazolium bromide) (Biomatik, Wilmington, DE) assays were performed by plating 7,500 cells/well in 10%FBS/DMEM in a 96-well plate, followed by incubation at 37^{o}C for 24 h. Cells were then treated with vehicle or increasing concentrations of

tcyDTDO, dMtcyDTDO, or dFtcyDTDO and incubated at 37°C for 72 h. Cell media was subsequently removed from each well and MTT assays were initiated by incubating cells with 0.5 mg/ml MTT in PBS for 3 h, followed by removal of the MTT solution and addition of 100 μL of DMSO to each well for 30 min. Absorbance of the MTT formazan product was subsequently measured at 570 and 690(reference) nm in a plate reader.

In vivo tumor studies and histochemical analysis

Breast cancer liver metastasis was initiated in NOD-SCID-gamma (NSG) mice obtained from Jackson Laboratories (Bar Harbor, ME) by injecting 1×10^6 cancer cells into the #4 mammary fat pads as described previously [4]. Mice bearing HCI-001/LVM2 breast tumors were treated once daily for four consecutive days with 20 mg/kg tcyDTDO by oral gavage and livers were collected. Animals bearing HER2+ BT474 tumors [2] were treated with the vehicle or 20 mg/kg dMtcyDTDO or dFtcyDTDO by intraperitoneal injection for four consecutive days. Tissue samples fixed in 4% paraformaldehyde/PBS and paraffin-embedded were sectioned and stained with hematoxylin and eosin (H&E) by the University of Florida Molecular Pathology Core (https://molecular.pathology.ufl.edu/).

Streptavidin-Agarose Pulldowns

Cells were treated with Biotin-PyrDTDO with or without Q-VD-OPH (MedChemExpress, Monmouth Junction, NJ) for 16 h in 10% FBS–DMEM, followed by the addition of 25 mM *N*-ethylmaleimide (NEM) (Thermo Scientific, Rockford, IL) for 20 min at 37°C. Cells were subsequently scraped directly into the media, washed twice with ice-cold PBS, and pelleted by centrifugation. Cells were extracted in buffer (20 mM HEPES (pH 7.4), 1 mM EDTA, 1mM EGTA, 5% Glycerol, 1 nM Microcystin, 1 mM Na_3VO_4, and 40 mM $Na_2H_2P_2O_7$) containing 1% Triton X-100. Samples were sonicated, followed by centrifugation for 20 min at 4°C. The supernatant was pre-cleared with Sepharose CL-6B (Amersham Biosciences AP, Uppsala, Sweden) for 2h at 4°C. Pre-cleared samples were then incubated with

Streptavidin (SA)-Agarose (Thermo Scientific, Rockford IL) and mixed on a Nutator for 24 h at 4^{o}C. SA-Agarose was washed three times with extraction buffer containing 0.1% Triton X-100, followed by the addition of 2X-SDS Sample buffer containing 2 mM biotin. Samples were analyzed by immunoblot, silver stain, or probing with Streptavidin-Alkaline Phosphatase.

Disulfide Bond-mediated Oligomerization

To assess protein disulfide bond-mediated oligomerization, cells were treated with DDAs for 24 h in 10% FBS–DMEM. Cells were subsequently scraped directly into the media and pelleted by centrifugation. Cells were extracted directly into boiling 2X-SDS-Sample Buffer containing 100 mM NEM and boiled for 10 min. Samples were sonicated, followed by centrifugation for 20 min at room temperature. Samples were subsequently analyzed by SDS-PAGE and immunoblot.

Surface Biotinylation

Cell surface proteins were labeled by incubation of cells with 1.6 mM Sulfo-NHS-SS-Biotin (Thermo Fisher Scientific, Waltham, MA) or 1.6 mM Biotin-dPEG$_3$-Maleimide (MilliporeSigma, St. Louis, MO) in Phosphate-Buffered Saline (PBS), pH 8.0 for 30 minutes at 4 °C. The cells were subsequently washed three times with PBS, and proteins were extracted in a buffer containing 1% Triton X-100 extraction buffer in the absence of reducing agents. Cell extracts were then incubated with Streptavidin-agarose beads (Thermo Fisher Scientific, Waltham, MA) for 2.5 h at 4^{o}C. Following centrifugation, the supernatant containing non-biotinylated proteins (flow-through) was retained and boiled in 2X-SDS-Sample Buffer containing 1% 2-mercaptoethanol. Streptavidin-agarose beads bound to biotinylated proteins were washed four times with 0.1% Triton X-100 extraction buffer, followed by boiling in 2X-SDS-Sample Buffer containing 1% 2-mercaptoethanol. Samples were then analyzed by immunoblot or blotting with Streptavidin-Alkaline Phosphatase.

Construction of AGR2 Vectors

Total RNA from BT474 cells was extracted with TRIzol Reagent (Invitrogen, Waltham, MA) according to the manufacturer's protocol. Total cellular RNA was used to synthesize first-strand cDNA by using the PCR conditions listed: 25□°C for 10□min, 42□°C for 30□min, and 95□°C for 5□min. PCR was subsequently performed using the following AGR2 primers: 5′-TTTTGGATCCCACCATGGAGAAAATTCCAGTG -3′ and 5′-TTTTTACGTATTACAATTCAGTCTTCAG-3′. The PCR fragment encoding AGR2 was subsequently digested with BamHI and SnaBI and cloned into the 5' BamHI and 3' SnaBI sites of pMXs-IRES-Blasticidin. The AGR2/pMXs-IRES-Blasticidin vector was used as a template for PCR reactions using the following AGR2 primers to amplify the DNA sequence downstream of the AGR2 signal sequence and to add 5'-BamHI and 3'-SalI sites: 5'-TTTTGGATCCCAGAGATACCACAGTCAAAC-3' and 5'-TTTTGTCGACTTACAATTCAGTCTTC-3'. The PCR fragment was digested with BamHI and SalI and cloned into the 5' BamHI and 3' SalI sites of pET-45b(+) (Novagen Burlington, MA). QuikChange mutagenesis was performed to produce the C81S mutation of AGR2 using the follow primers: 5'-CATCACTTGGATGAGTCCCCACACAGTCAAGC-3' and 5'-GCTTGACTGTGTGGGGACTCATCCAAGTGATG-3'. The C81S mutation of AGR2 was verified by sequencing.

His_6-AGR2 TALON Purification

Competent BL21(DE3) cells were transformed with either the AGR2/pET-45b(+) or AGR2 C81S/pET-45b(+) vectors. Protein expression was induced by the addition of 50 μM Isopropyl β- D -1-thiogalactopyranoside (Fisher Scientific, Fair Lawn, NJ) to bacterial cell cultures for 2.5 hours and shaking at 37^{o}C. Bacterial cells were subsequently pelleted and dissolved in Mouse Tonicity Phosphate Buffered Saline (MTPBS) containing 1% Triton X-100 and sonicated for 20 seconds on ice, followed by centrifugation for 10 min at 4^{o}C to pellet cell debris. The supernatant was transferred

to a new tube, followed by the addition of TALON Resin (Clontech, Mountain View, CA) and mixing on a Nutator for 30 min at 4^{o}C. The TALON Resin was pelleted by centrifugation and washed twice with MTPBS and twice with MTPBS containing 30 mM Imidazole. Protein bound to the TALON Resin was eluted with 400 mM Imidazole and precipitated with 60% saturated ammonium sulfate. The precipitated protein was pelleted by centrifugation, dissolved in MTPBS containing 1 mM DTT and 1 mM EDTA, and subsequently dialyzed against a solution of MTPBS containing 10 μM DTT and 30% Glycerol.

DDA-AGR2 Binding Experiments

Purified His_6-AGR2 or His_6-AGR2 C81S, as prepared above, or His_6-AGR2 (PRO-580) or His_6-AGR3 (PRO-242) obtained from ProSpec (New Brunswick NJ) were incubated with or without varying concentrations of the unlabeled DDA competitors, tcyDTDO or dMtcyDTDO, and 30 μM Biotin-GlyPyrDTDO or Biotin-PyrDTDO in buffer (20 mM HEPES (pH 7.4), 1 mM EDTA, 1mM EGTA, 5% Glycerol, 1 nM Microcystin, 1 mM Na_3VO_4, and 40 mM $Na_2H_2P_2O_7$) containing 1% Triton-X 100 for 30 min at 37^{o}C. Preliminary studies showed that Biotin-GlyPyrDTDO or Biotin-PyrDTDO exhibited indistinguishable labeling of proteins in intact cells and purified proteins in vitro. Therefore, the two probes were used interchangeably. Reactions were stopped by boiling the samples in 2X-SDS-Sample Buffer containing 100 mM NEM for 10 min. Biotin-DDA labeling of protein was verified by blotting with Streptavidin-Alkaline Phosphatase (Rockland Immunochemicals, Inc., Limerick, PA). ERp44 (PRO-547) and PDIA1 (ENZ-262) were obtained from ProSpec and used in experiments examining the binding of these proteins to Biotin-PyrDTDO.

Sample Preparation for Mass Spectrometry

Total proteins were solubilized in 50 mM NH_4HCO_3 pH 8.5, and Trypsin (Promega, Fitchburg, WI) was added for digestion (w/w for enzyme : sample = 1 : 100) overnight at 37 °C. The digested

peptides were desalted using micro ZipTip mini-reverse phase (Millipore), and then lyophilized to dryness.

Nano-LC-MS

Peptides derived from the protein samples were suspended in 0.1% formic acid for mass spectrometric analysis. The bottom-up proteomics data acquisition was performed on an EASY-nLC 1200 ultra-performance liquid chromatography system connected to an Orbitrap Fusion Tribrid instrument equipped with a nano-electrospray source (Thermo Scientific, San Jose, CA). The peptide samples were loaded onto a C18 trapping column (75 µm i.d. × 2 cm, Acclaim PepMap® 100 particles with 3 µm size and 100 Å pores) and eluted onto a C18 analytical column (75 µm i.d. x 25 cm, 2 µm particles with 100 Å pore size). The flow rate was set at 300 nL/minute with solvent A (0.1% formic acid in water) and solvent B (0.1% formic acid and 99.9% acetonitrile) as the mobile phases. Separation was conducted using the following gradient: 2% of B over 0 – 0.5 min; 2 - 35 % of B over 0.5 - 45 min, 35 - 98 % of B over 45 - 46 min, and isocratic at 98% of B over 46-59 min, and then from 98 – 2% of B from 59 – 60 min. The equilibration time at 2% B is 15 min.

An Orbitrap with a resolution of 120,000 at m/z 400 was used for a full MS1 scan (m/z 350 - 2000). The automatic gain control (AGC) target is 2e5 with 50 ms as the maximum injection time. Monoisotopic precursor selection (MIPS) was enforced to filter for peptides. Peptides bearing +2 - 6 charges were selected with an intensity threshold of 1e4. Dynamic exclusion of 15 s was used to prevent resampling of high abundance peptides. Top speed method was used for data dependent acquisition within a cycle of 3 s. The MS/MS was carried out in the ion trap, with a quadrupole isolation window of 1.3 Da. Fragmentation of the selected peptides by collision-induced dissociation (CID) was done at 35% of normalized collision energy with 10 ms activation time. The MS2 spectra were detected in the linear ion trap with the AGC target as 1e4 and the maximum injection time as 35 ms.

Database searching was performed on all MS/MS samples using Mascot (Matrix Science, London, UK; version 2.4.1), with a fragment ion mass tolerance of 0.50 Da, a parent ion tolerance of 10.0 PPM. Mascot was set up to search the IPI_human database assuming the digestion enzyme trypsin. MS/MS based peptide and protein identifications were made with Scaffold (version Scaffold_4.2.1, Proteome Software Inc., Portland, OR). Peptide Prophet algorithm [64] with Scaffold delta-mass correction was utilized to accept peptide identification at greater than 95.0% probability. Protein identifications were accepted if they contained a minimum of 1 identified peptide and could be established at greater than 95.0% probability. The Protein Prophet algorithm [65] was utilized to assign protein probabilities. Proteins were grouped into clusters if they shared significant peptide evidence.

Statistics

Student's t-test was used for comparisons in both in vitro and in vivo experiments. All P values are two-tailed, and both P values and statistical tests are mentioned in either figures or legends. Points plotted on line graphs are the average of six or more technical replicates and are representative of three or more independent biological replicates. Error bars represent standard deviation of the mean. Immunoblot analyses are representative of at least three independent replicates with similar results.

Chemical Synthesis of DDAs

Full experimental and characterization details associated with the synthesis of (±)-BocPyrDTDO, Biotin-GlyPyrDTDO, and Biotin-PyrDTDO are provided in the Supplemental Information. Detailed discussion of the syntheses and analytical characterization of dMtcyDTDO and dFtcyDTDO will be published elsewhere.

Acknowledgements

These studies were supported in part by grants from the Florida Breast Cancer Foundation (BL and RC), the Ocala Royal Dames for Cancer Research (BL), and the Office of the Assistant Secretary of Defense for Health Affairs through the Breast Cancer Research Program under Award Nos. W81XWH-15-1-0199 (BL) and W81XWH-15-1-0200 (RC), and NIH/NCI grant CA252400 (BL). RF is grateful to the University of Florida for a Graduate School Fellowship and EY thanks the Dr. Howard and Brenda Sheridan Fund in Chemistry for a 2020 Howard and Brenda Sheridan Summer Fellowship. Mass spectrometric data on DDA protein targets were obtained by the Proteomics and Mass Spectrometry Facility at the Interdisciplinary Center for Biotechnology Research. Mass spectrometric data on DDA compound structures and DDA adducts were obtained by the UF Department of Chemistry Mass Spectrometry Research and Education Center supported, in part, by the National Institutes of Health (NIH S10 OD021758-01A1).

Author Contributions

Brian Law, Ronald Castellano, and Mary Law designed the studies. Cell culture, in vitro DDA binding assays, and tumor studies were carried out by Brian Law, Bradley Davis, and Mary Law. Synthesis, purification, analysis, and characterization of the DDA compounds were carried out by Elham Yaaghubi, Amanda Ghilardi, Renan Ferreira, Sadie DePeter, and Christopher Schilson. Mass spectrometry studies and their analysis were carried out by Jin Koh and Sixue Chen. Coy Heldermon provided tumor models and contributed to the planning of the tumor studies and the analysis of the results. Peter Nørgaard assisted with the interpretation of tumor pathology. Chi-Wu Chiang and all other Authors read and participated in the writing and/or editing of the manuscript.

Conflict of Interest

Brian Law and Ronald Castellano are inventors on issued and pending patents related to the DDA compounds and are founding members of Quattro Therapeutics, LLC.

The paper explained

Problem

DDAs are a novel class of anticancer agents, but their mechanisms of action are not well understood because the direct DDA target proteins in cancer cells have not been identified.

Results

Herein, we identify the PDI-family members AGR2, AGR3, ERp44, and PDIA1 as direct DDA target proteins and show that these DDA targets mediate the ability of DDAs to induce the oligomerization and activation of DR4/5, and the parallel oligomerization and downregulation of EGFR/HER2/HER3.

Impact

Small molecule therapeutics that inhibit the functions of AGR2/3 and ERp44 by binding to their active site Cysteine residues have not been previously identified and ERp44 has not been investigated as a target for anticancer agents. Thus, DDAs provide a new mechanistic strategy to target cancer cells by altering the disulfide bonding patterns of key AGR2, ERp44, and PDIA1 client proteins that include DR4/5 and EGFR/HER2/HER3.

References

1 DeSantis CE, Ma J, Gaudet MM, Newman LA, Miller KD, Goding Sauer A *et al*. Breast cancer statistics, 2019. *CA Cancer J Clin* 2019; 69: 438-451.

2 Ferreira RB, Law ME, Jahn SC, Davis BJ, Heldermon CD, Reinhard M *et al*. Novel agents that downregulate EGFR, HER2, and HER3 in parallel. *Oncotarget* 2015; 6: 10445-10459.

3 Ferreira RB, Wang M, Law ME, Davis BJ, Bartley AN, Higgins PJ *et al*. Disulfide bond disrupting agents activate the unfolded protein response in EGFR- and HER2-positive breast tumor cells. *Oncotarget* 2017; 8: 28971-28989.

4 Wang M, Law ME, Davis BJ, Yaaghubi E, Ghilardi AF, Ferreira RB *et al*. Disulfide bond-disrupting agents activate the tumor necrosis family-related apoptosis-inducing ligand/death receptor 5 pathway. *Cell Death Discovery* 2019; 5: 153.

5 Wiley SR, Schooley K, Smolak PJ, Din WS, Huang CP, Nicholl JK *et al*. Identification and characterization of a new member of the TNF family that induces apoptosis. *Immunity* 1995; 3: 673-682.

6 Rieger J, Naumann U, Glaser T, Ashkenazi A, Weller M. APO2 ligand: a novel lethal weapon against malignant glioma? *FEBS Lett* 1998; 427: 124-128.

7 Zamai L, Ahmad M, Bennett IM, Azzoni L, Alnemri ES, Perussia B. Natural killer (NK) cell-mediated cytotoxicity: differential use of TRAIL and Fas ligand by immature and mature primary human NK cells. *J Exp Med* 1998; 188: 2375-2380.

8 Ashkenazi A, Pai RC, Fong S, Leung S, Lawrence DA, Marsters SA *et al*. Safety and antitumor activity of recombinant soluble Apo2 ligand. *J Clin Invest* 1999; 104: 155-162.

9 Thapa B, Kc R, Uludag H. TRAIL therapy and prospective developments for cancer treatment. *J Control Release* 2020; 326: 335-349.

10 Wang M, Law ME, Davis BJ, Yaaghubi E, Ghilardi AF, Ferreira RB *et al*. Mechanistic Elucidation of the Antitumor Properties of a Novel Death Receptor 5 Activator. *bioRxiv* 2019: 700906.

11 Pan L, Fu TM, Zhao W, Zhao L, Chen W, Qiu C *et al*. Higher-Order Clustering of the Transmembrane Anchor of DR5 Drives Signaling. *Cell* 2019; 176: 1477-1489 e1414.

12 Dong A, Wodziak D, Lowe AW. Epidermal growth factor receptor (EGFR) signaling requires a specific endoplasmic reticulum thioredoxin for the post-translational control of receptor presentation to the cell surface. *J Biol Chem* 2015; 290: 8016-8027.

13 Park SW, Zhen G, Verhaeghe C, Nakagami Y, Nguyenvu LT, Barczak AJ *et al*. The protein disulfide isomerase AGR2 is essential for production of intestinal mucus. *Proc Natl Acad Sci U S A* 2009; 106: 6950-6955.

14 Schroeder BW, Verhaeghe C, Park SW, Nguyenvu LT, Huang X, Zhen G *et al*. AGR2 is induced in asthma and promotes allergen-induced mucin overproduction. *Am J Respir Cell Mol Biol* 2012; 47: 178-185.

15 Galligan JJ, Petersen DR. The human protein disulfide isomerase gene family. *Hum Genomics* 2012; 6: 6.

16 Shergalis AG, Hu S, Bankhead A, 3rd, Neamati N. Role of the ERO1-PDI interaction in oxidative protein folding and disease. *Pharmacol Ther* 2020; 210: 107525.

17 Laboissiere MC, Sturley SL, Raines RT. The essential function of protein-disulfide isomerase is to unscramble non-native disulfide bonds. *J Biol Chem* 1995; 270: 28006-28009.

18 Hampe L, Radjainia M, Xu C, Harris PW, Bashiri G, Goldstone DC *et al*. Regulation and Quality Control of Adiponectin Assembly by Endoplasmic Reticulum Chaperone ERp44. *J Biol Chem* 2015; 290: 18111-18123.

19 Long Q, Lei T, Feng B, Yin C, Jin D, Wu Y *et al*. Peroxisome proliferator-activated receptor-gamma increases adiponectin secretion via transcriptional repression of endoplasmic reticulum chaperone protein ERp44. *Endocrinology* 2010; 151: 3195-3203.

20 Cortini M, Sitia R. From antibodies to adiponectin: role of ERp44 in sizing and timing protein secretion. *Diabetes Obes Metab* 2010; 12 Suppl 2: 39-47.

21 Cortini M, Sitia R. ERp44 and ERGIC-53 synergize in coupling efficiency and fidelity of IgM polymerization and secretion. *Traffic* 2010; 11: 651-659.

22 Otsu M, Bertoli G, Fagioli C, Guerini-Rocco E, Nerini-Molteni S, Ruffato E *et al*. Dynamic retention of Ero1alpha and Ero1beta in the endoplasmic reticulum by interactions with PDI and ERp44. *Antioxid Redox Signal* 2006; 8: 274-282.

23 Yang K, Li DF, Wang X, Liang J, Sitia R, Wang CC *et al*. Crystal Structure of the ERp44-Peroxiredoxin 4 Complex Reveals the Molecular Mechanisms of Thiol-Mediated Protein Retention. *Structure* 2016; 24: 1755-1765.

24 Fraldi A, Zito E, Annunziata F, Lombardi A, Cozzolino M, Monti M *et al*. Multistep, sequential control of the trafficking and function of the multiple sulfatase deficiency gene product, SUMF1 by PDI, ERGIC-53 and ERp44. *Hum Mol Genet* 2008; 17: 2610-2621.

25 Hisatsune C, Ebisui E, Usui M, Ogawa N, Suzuki A, Mataga N *et al*. ERp44 Exerts Redox-Dependent Control of Blood Pressure at the ER. *Mol Cell* 2015; 58: 1015-1027.

26 Tempio T, Anelli T. The pivotal role of ERp44 in patrolling protein secretion. *J Cell Sci* 2020; 133.

27 Lemmon MA, Schlessinger J. Cell signaling by receptor tyrosine kinases. *Cell* 2010; 141: 1117-1134.

28 Cha SS, Sung BJ, Kim YA, Song YL, Kim HJ, Kim S *et al*. Crystal structure of TRAIL-DR5 complex identifies a critical role of the unique frame insertion in conferring recognition specificity. *J Biol Chem* 2000; 275: 31171-31177.

29 Wang MX, Ferreira RB, Law ME, Davis BJ, Yaaghubi E, Ghilardi AF *et al*. A novel proteotoxic combination therapy for EGFR+ and HER2+cancers. *Oncogene* 2019; 38: 4264-4282.

30 DeRose YS, Gligorich KM, Wang G, Georgelas A, Bowman P, Courdy SJ *et al*. Patient-derived models of human breast cancer: protocols for in vitro and in vivo applications in tumor biology and translational medicine. *Curr Protoc Pharmacol* 2013; Chapter 14: Unit14 23.

31 Bondi A. Van Der Waals Volumes + Radii. *J Phys Chem-Us* 1964; 68: 441-+.

32 Gillis EP, Eastman KJ, Hill MD, Donnelly DJ, Meanwell NA. Applications of Fluorine in Medicinal Chemistry. *Journal of Medicinal Chemistry* 2015; 58: 8315-8359.

33 Wang J, Sanchez-Rosello M, Acena JL, del Pozo C, Sorochinsky AE, Fustero S *et al*. Fluorine in Pharmaceutical Industry: Fluorine-Containing Drugs Introduced to the Market in the Last Decade (2001-2011). *Chemical Reviews* 2014; 114: 2432-2506.

34 Park BK, Kitteringham NR, O'Neill PM. Metabolism of fluorine-containing drugs. *Annu Rev Pharmacol* 2001; 41: 443-470.

35 Frand AR, Kaiser CA. The ERO1 gene of yeast is required for oxidation of protein dithiols in the endoplasmic reticulum. *Mol Cell* 1998; 1: 161-170.

36 Pollard MG, Travers KJ, Weissman JS. Ero1p: a novel and ubiquitous protein with an essential role in oxidative protein folding in the endoplasmic reticulum. *Mol Cell* 1998; 1: 171-182.

37 Bertoli G, Simmen T, Anelli T, Molteni SN, Fesce R, Sitia R. Two conserved cysteine triads in human Ero1alpha cooperate for efficient disulfide bond formation in the endoplasmic reticulum. *J Biol Chem* 2004; 279: 30047-30052.

38 Sannino S, Anelli T, Cortini M, Masui S, Degano M, Fagioli C *et al*. Progressive quality control of secretory proteins in the early secretory compartment by ERp44. *J Cell Sci* 2014; 127: 4260-4269.

39 Law ME, Ferreira RB, Davis BJ, Higgins PJ, Kim JS, Castellano RK *et al*. CUB domain-containing protein 1 and the epidermal growth factor receptor cooperate to induce cell detachment. *Breast Cancer Res* 2016; 18: 80.

40 Wang M, Law ME, Davis BJ, Yaaghubi E, Ghilardi AF, Ferreira RB *et al*. Disulfide bond-disrupting agents activate the tumor necrosis family-related apoptosis-inducing ligand/death receptor 5 pathway. *Cell Death Discov* 2019; 5: 153.

41 Stockhausen MT, Broholm H, Villingshoj M, Kirchhoff M, Gerdes T, Kristoffersen K *et al*. Maintenance of EGFR and EGFRvIII expressions in an in vivo and in vitro model of human glioblastoma multiforme. *Exp Cell Res* 2011; 317: 1513-1526.

42 Cho J, Pastorino S, Zeng Q, Xu X, Johnson W, Vandenberg S *et al*. Glioblastoma-derived epidermal growth factor receptor carboxyl-terminal deletion mutants are transforming and are sensitive to EGFR-directed therapies. *Cancer Res* 2011; 71: 7587-7596.

43 Liu D, He J, Yuan Z, Wang S, Peng R, Shi Y *et al*. EGFR expression correlates with decreased disease-free survival in triple-negative breast cancer: a retrospective analysis based on a tissue microarray. *Med Oncol* 2012; 29: 401-405.

44 de Ruijter TC, Veeck J, de Hoon JP, van Engeland M, Tjan-Heijnen VC. Characteristics of triple-negative breast cancer. *J Cancer Res Clin Oncol* 2011; 137: 183-192.

45 Toyama T, Yamashita H, Kondo N, Okuda K, Takahashi S, Sasaki H *et al*. Frequently increased epidermal growth factor receptor (EGFR) copy numbers and decreased BRCA1 mRNA expression in Japanese triple-negative breast cancers. *BMC Cancer* 2008; 8: 309.

46 Stojak M, Milczarek M, Kurpinska A, Suraj-Prazmowska J, Kaczara P, Wojnar-Lason K *et al*. Protein Disulphide Isomerase A1 Is Involved in the Regulation of Breast Cancer Cell Adhesion and Transmigration via Lung Microvascular Endothelial Cells. *Cancers (Basel)* 2020; 12.

47 Xu S, Liu Y, Yang K, Wang H, Shergalis A, Kyani A *et al*. Inhibition of protein disulfide isomerase in glioblastoma causes marked downregulation of DNA repair and DNA damage response genes. *Theranostics* 2019; 9: 2282-2298.

48 Gupta A, Dong A, Lowe AW. AGR2 gene function requires a unique endoplasmic reticulum localization motif. *J Biol Chem* 2012; 287: 4773-4782.

49 Guo H, Zhu Q, Yu X, Merugu SB, Mangukiya HB, Smith N *et al*. Tumor-secreted anterior gradient-2 binds to VEGF and FGF2 and enhances their activities by promoting their homodimerization. *Oncogene* 2017; 36: 5098-5109.

50 Jia M, Guo Y, Zhu D, Zhang N, Li L, Jiang J *et al*. Pro-metastatic activity of AGR2 interrupts angiogenesis target bevacizumab efficiency via direct interaction with VEGFA and activation of NF-kappaB pathway. *Biochim Biophys Acta Mol Basis Dis* 2018; 1864: 1622-1633.

51 Arumugam T, Deng D, Bover L, Wang H, Logsdon CD, Ramachandran V. New Blocking Antibodies against Novel AGR2-C4.4A Pathway Reduce Growth and Metastasis of Pancreatic Tumors and Increase Survival in Mice. *Mol Cancer Ther* 2015; 14: 941-951.

52 Liu AY, Kanan AD, Radon TP, Shah S, Weeks ME, Foster JM *et al*. AGR2, a unique tumor-associated antigen, is a promising candidate for antibody targeting. *Oncotarget* 2019; 10: 4276-4289.

53 Eriksson O, Stopa J, Furie B. Identification of PDI Substrates by Mechanism-Based Kinetic Trapping. *Methods Mol Biol* 2019; 1967: 165-182.

54 Stopa JD, Baker KM, Grover SP, Flaumenhaft R, Furie B. Kinetic-based trapping by intervening sequence variants of the active sites of protein-disulfide isomerase identifies platelet protein substrates. *J Biol Chem* 2017; 292: 9063-9074.

55 Wang ZV, Schraw TD, Kim JY, Khan T, Rajala MW, Follenzi A *et al*. Secretion of the adipocyte-specific secretory protein adiponectin critically depends on thiol-mediated protein retention. *Mol Cell Biol* 2007; 27: 3716-3731.

56 Wolf G. New insights into thiol-mediated regulation of adiponectin secretion. *Nutr Rev* 2008; 66: 642-645.

57 Anelli T, Ceppi S, Bergamelli L, Cortini M, Masciarelli S, Valetti C *et al*. Sequential steps and checkpoints in the early exocytic compartment during secretory IgM biogenesis. *EMBO J* 2007; 26: 4177-4188.

58 DeRose YS, Wang G, Lin YC, Bernard PS, Buys SS, Ebbert MT *et al*. Tumor grafts derived from women with breast cancer authentically reflect tumor pathology, growth, metastasis and disease outcomes. *Nat Med* 2011; 17: 1514-1520.

59 Law BK, Chytil A, Dumont N, Hamilton EG, Waltner-Law ME, Aakre ME *et al*. Rapamycin potentiates transforming growth factor beta-induced growth arrest in nontransformed, oncogene-transformed, and human cancer cells. *Mol Cell Biol* 2002; 22: 8184-8198.

60 Law ME, Corsino PE, Jahn SC, Davis BJ, Chen S, Patel B *et al*. Glucocorticoids and histone deacetylase inhibitors cooperate to block the invasiveness of basal-like breast cancer cells through novel mechanisms. *Oncogene* 2013; 32: 1316-1329.

61 Corsino P, Horenstein N, Ostrov D, Rowe T, Law M, Barrett A *et al*. A novel class of cyclin-dependent kinase inhibitors identified by molecular docking act through a unique mechanism. *J Biol Chem* 2009; 284: 29945-29955.

62 Law BK, Norgaard P, Moses HL. Farnesyltransferase inhibitor induces rapid growth arrest and blocks p70s6k activation by multiple stimuli. *J Biol Chem* 2000; 275: 10796-10801.

63 Law BK, Waltner-Law ME, Entingh AJ, Chytil A, Aakre ME, Norgaard P *et al*. Salicylate-induced growth arrest is associated with inhibition of p70s6k and down-regulation of c-myc, cyclin D1, cyclin A, and proliferating cell nuclear antigen. *J Biol Chem* 2000; 275: 38261-38267.

64 Keller A, Nesvizhskii AI, Kolker E, Aebersold R. Empirical statistical model to estimate the accuracy of peptide identifications made by MS/MS and database search. *Anal Chem* 2002; 74: 5383-5392.

65 Nesvizhskii AI, Keller A, Kolker E, Aebersold R. A statistical model for identifying proteins by tandem mass spectrometry. *Anal Chem* 2003; 75: 4646-4658.

Figure Legends

Figure 1 - DDAs induce rapid tumor regression and exhibit oral activity against metastatic disease.

A. Representative first and second generation DDAs (RBF3, DTDO, and tcyDTDO) and illustration of interconversion between the linear and cyclic forms of the DDA pharmacophore.

B. Mice bearing HCI-001/LVM2 breast tumors and associated liver metastases were treated once daily for four days with 20 mg/kg tcyDTDO. Livers were collected and stained with hematoxylin and eosin (H&E).

C. Structures of new tcyDTDO derivatives dMtcyDTDO and dFtcyDTDO.

D. MDA-MB-468 cells were treated for 24 h with the indicated concentrations of DDAs and cell viability (MTT) assays were performed.

E. MDA-MB-468 cells were treated for 24 h as indicated and subjected to immunoblot analysis after non-reducing SDS-PAGE. O and M represent disulfide bonded oligomeric and monomeric protein forms, respectively.

F. Mice bearing BT474 cell xenograft tumors were treated once daily for five days with vehicle, 20 mg/kg dFtcyDTDO, or 20 mg/kg dMtcyDTDO. Two hours after the final treatment, mammary fat pads/tumors were excised and tumor sections were stained with H&E. T denotes tumor tissue, FP indicates mammary fat pads, and CN represents coagulation necrosis.

Figure 2 - AGR2 and AGR3 are DDA target proteins.

A. Abbreviated synthetic approach and chemical structures of the biotinylated DDA analogs Biotin-PyrDTDO and Biotin-GlyPyrDTDO.

B. Purified, recombinant AGR2 was reacted with Biotin-GlyPyrDTDO for 1 h at 37°C, resolved by non-reducing SDS-PAGE, transferred to membranes, and probed with Streptavidin-Alkaline Phosphatase, and by anti-AGR2 immunoblot.

C. Vector control or AGR2 knockdown MDA-MB-468 cells were treated for 24 h as indicated and analyzed by non-reducing (left panels) or reducing (right panels) immunoblot (CC8, Cleaved Caspase 8). Red arrow indicates oligomerized forms of DR5 that are present at higher levels in the AGR2 knockdown cells. O and M represent disulfide bonded oligomeric and monomeric protein forms, respectively.

D. Biotin-GlyPyrDTDO binding assays performed as in Fig. 2B, employing the C81S AGR2 mutant and AGR3 in addition to AGR2. In the indicated samples, the proteins were pre-incubated with 600 μM dMtcyDTDO to determine if this prevented subsequent Biotin-GlyPyrDTDO binding.

E. AGR2 binding assay performed as in Fig. 2B to examine the relative abilities of pre-incubation of AGR2 with dMtcyDTDO or tcyDTDO to block subsequent binding of Biotin-GlyPyrDTDO.

Figure 3 - ERp44 and PDIA1 are additional DDA targets.

A. Breast cancer cell lines were treated for 16 h with vehicle, 100 μM Biotin-PyrDTDO, or 100 μM Biotin-PyrDTDO + 10 μM Q-VD-OPH for 16 h. Biotinylated proteins were isolated using Streptavidin-coated beads and the crude extracts and Streptavidin pulldowns were analyzed by blotting with Streptavidin-Alkaline Phosphatase. Red arrows indicate bands, designated DDAT1 and DDAT2, present exclusively after Biotin-PyrDTDO treatment.

B. Biotin-PyrDTDO/Streptavidin pulldowns were performed in BT474 and MDA-MB-468 cells. Purified material was analyzed by Streptavidin-Alkaline Phosphatase detection and silver stain.

C, left panel. The indicated breast cancer lines were treated with vehicle or 100 μM Biotin-PyrDTDO for 16 h and extracts were subjected to Streptavidin-agarose pulldowns, or anti-AGR2 or anti-ERp44 immunoprecipitations. The purified material was analyzed by immunoblot with the indicated antibodies. C, right panel. BT474 and MDA-MB-468 breast cancer lines were treated with vehicle or 100 μM Biotin-PyrDTDO for 16 h and extracts were subjected to Streptavidin-agarose pulldowns. The affinity-purified samples were analyzed by immunoblot.

D. Binding assays employing recombinant, purified ERp44 and PDIA1. Proteins were labeled with Biotin-PyrDTDO after pretreatment with vehicle or dMtcyDTDO. Reactions were analyzed by non-reducing SDS-PAGE followed by detection with Streptavidin-Alkaline Phosphatase.

E. MDA-MB-468 cells were treated or 24 h with vehicle (control) or 5 μM dMtcyDTDO. Cell extracts were resolved by non-reducing SDS-PAGE and analyzed by immunoblot with the indicated antibodies. O and M represent disulfide bonded oligomeric and monomeric protein forms, respectively (CC8, Cleaved Caspase 8). Red arrows denote bands stained with ERp44 or PDIA1 antibodies that change in abundance with dMtcyDTDO treatment.

Figure 4 - Evidence that disulfide bonding of DR4 and DR5 are regulated by ERp44.

A. Immunoblot analysis of the expression levels of EGFR, ERO1-α, AGR2, AGR3, PDIA1 and ERp44 across a panel of breast cancer cell lines. Actin serves as a loading control.

B. MDA-MB-468 cells were treated for 24 h with 10 μM dMtcyDTDO or vehicle and cell extracts were immunoprecipitated with ERp44 antibody and analyzed by immunoblot.

C. BT474 cells stably expressing ERp44 or transduced with the vector control were treated for 24 h with vehicle, 2.5 μM, or 5 μM dMtcyDTDO. Cell extracts were resolved by SDS-PAGE under non-reducing (left panel) or reducing (right panel) conditions and analyzed by immunoblot. O and M are disulfide bonded oligomeric and monomeric protein forms, respectively.

D, left panel. Vector control or ERp44 knockdown MDA-MB-468 cell lines were treated for 24 h with vehicle, 2.5 μM, or 5 μM dMtcyDTDO. Cell extracts were resolved by non-reducing SDS-PAGE and analyzed by immunoblot (CC8, Cleaved Caspase 8). O and M are disulfide bonded oligomeric and monomeric protein bands, respectively. D, right panel. Expanded portions of the blots from the left

panel showing bands at the stacking gel/resolving gel interface (SGI). Asterisks denote bands at the SGI that are more prominent in the shERp44 knockdown cells.

Figure 5 – Mutation of ERp44 thioredoxin-like repeat residues alters DDA responses.

A. Non-reducing immunoblot analysis of vector control MDA-MB-468 cells, or cells overexpressing wild type ERp44, ERp44[C58S], or ERp44[S61C]. O and M are disulfide bonded oligomeric and monomeric protein bands, respectively. M (FL) and M (Cl.) represent the monomeric full-length and cleaved forms of CDCP1, respectively.

B. Non-reducing immunoblot analysis of the indicated cell lines treated with vehicle or 7.5 μM dFtcyDTDO for 24 h. O and M are disulfide bonded oligomeric and monomeric protein bands, respectively.

C. Extracts from vector control or EGFR overexpressing T47D cells were analyzed by non-reducing SDS-PAGE followed by immunoblot. O and M are disulfide bonded oligomeric and monomeric protein bands, respectively.

D. MDA-MB-468 cells were treated for 24 h with vehicle or 2.5 μM dMtcyDTDO. The cells were then subjected to cell surface protein labeling using membrane-impermeable amine- or thiol-reactive biotinylation probes as described in Materials and Methods. Surface proteins were collected using Streptavidin-coated beads and analyzed along with the flow-though (internal, non-biotinylated proteins) by immunoblot.

Figure 6 - Models for the molecular mechanisms of DDA action.

A. DDAs act on the PDI-family proteins ERp44, AGR2/3, and PDIA1 to alter the disulfide bonding of DR4, DR5, and HER-family proteins. This results in upregulation of DR5, disulfide bond-mediated oligomerization of DR4 and DR5, accumulation of DR4/5 to the cell surface, and activation of the Caspase 8-Caspase 3 pro-apoptotic cascade. Disulfide mediated HER1-3 oligomerization is associated with their downregulation.

B. Thioredoxin-like repeat motifs of AGR2, AGR3, and ERp44.

C. Model for DDA target protein selectivity in which a thiolate-containing target protein reacts covalently with a DDA, liberating a sulfinate group. Solvation/stabilization of the sulfinate group is hypothesized to prevent DDA release from the protein by recyclization-mediated auto-excision.

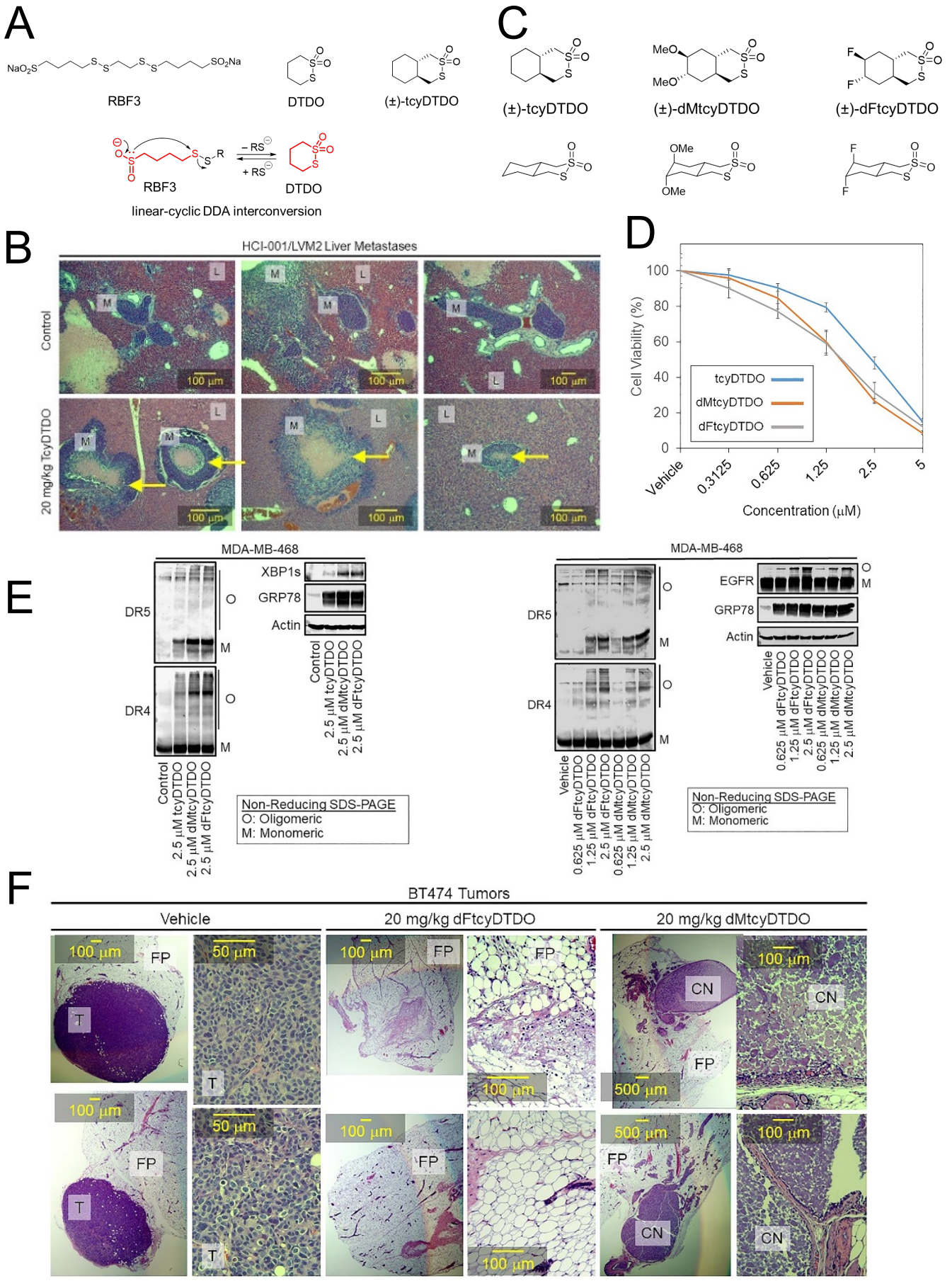

Fig. 1, Law et al.

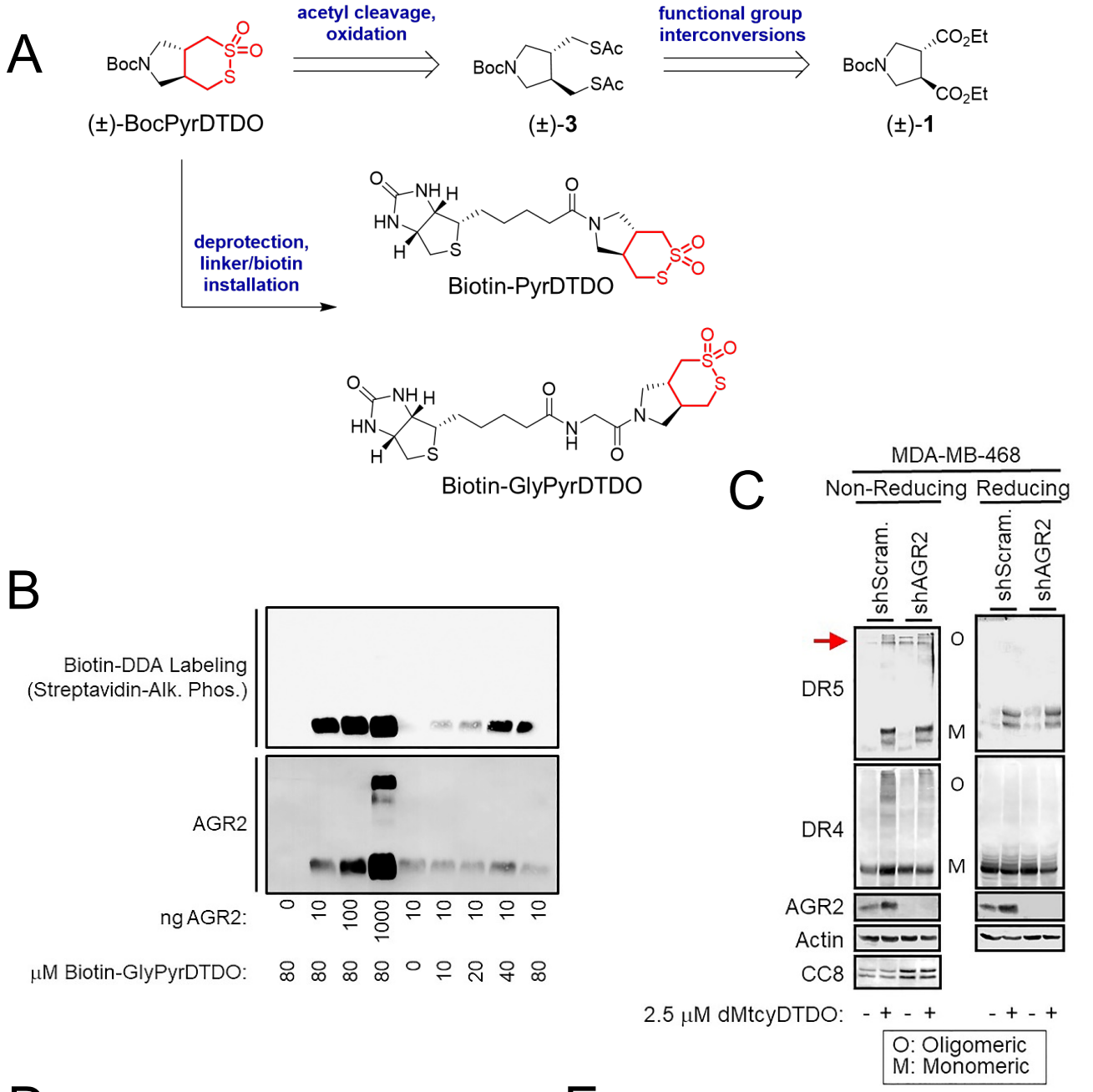

Fig. 2, Law et al.

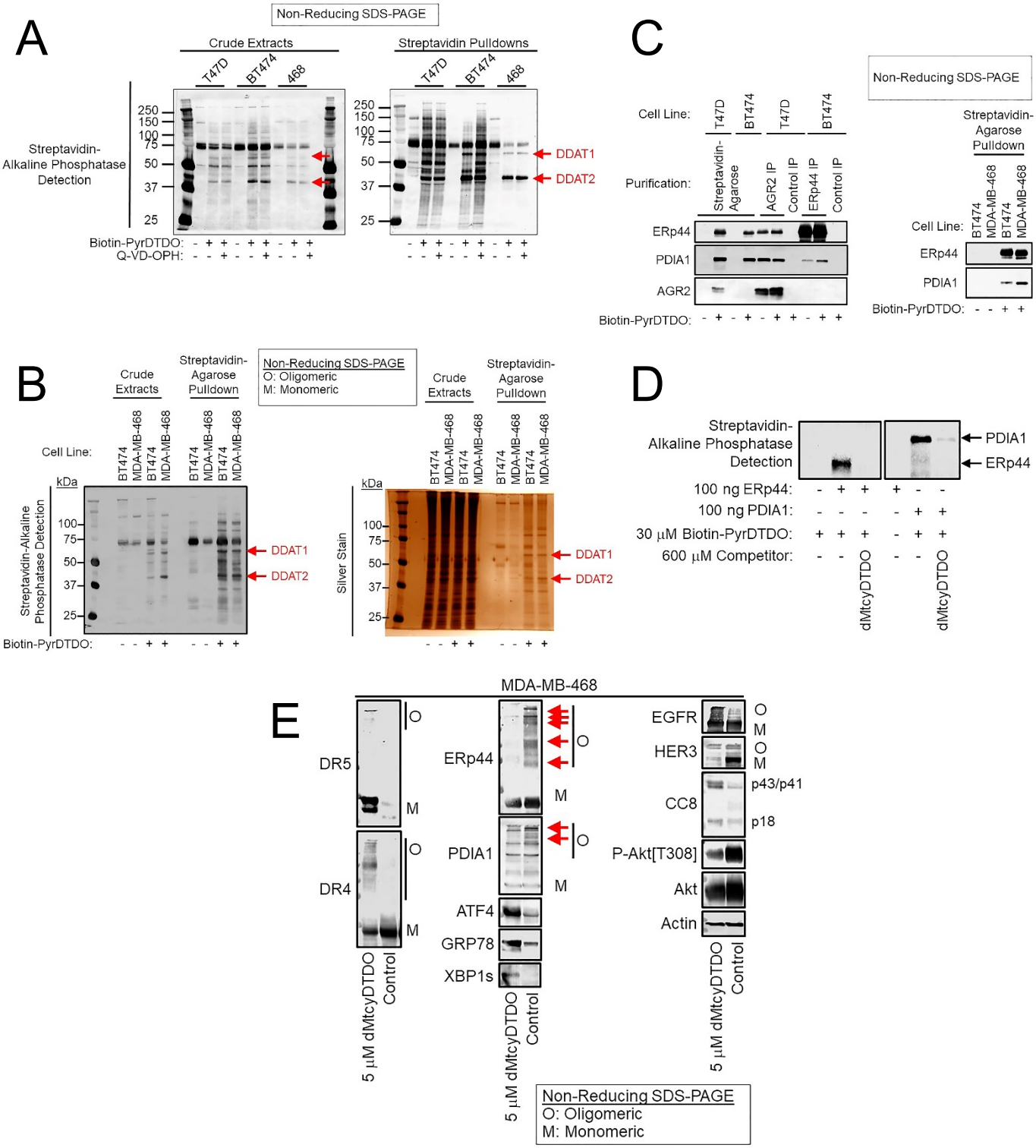

Fig. 3, Law et al.

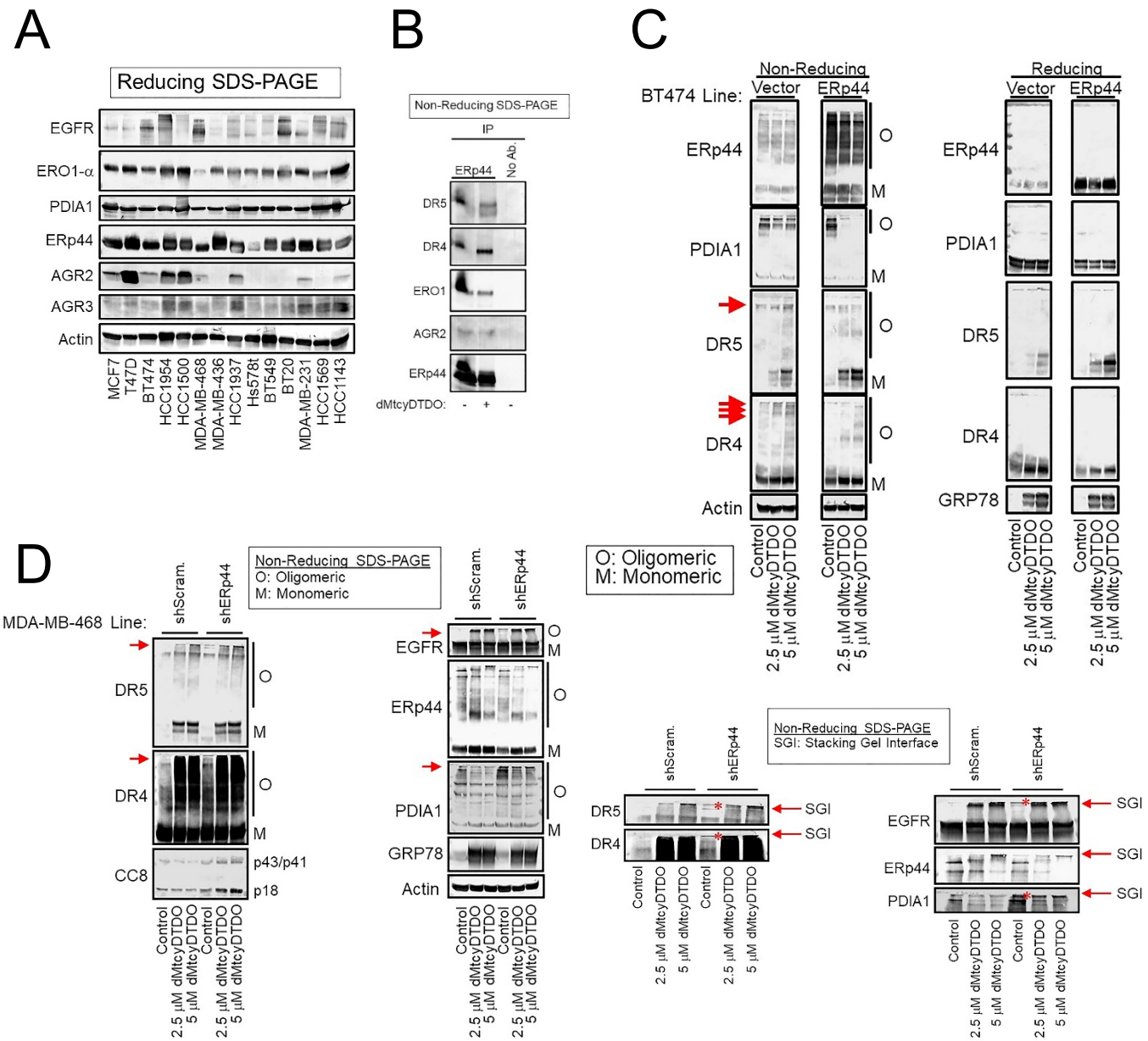

Fig. 4, Law et al.

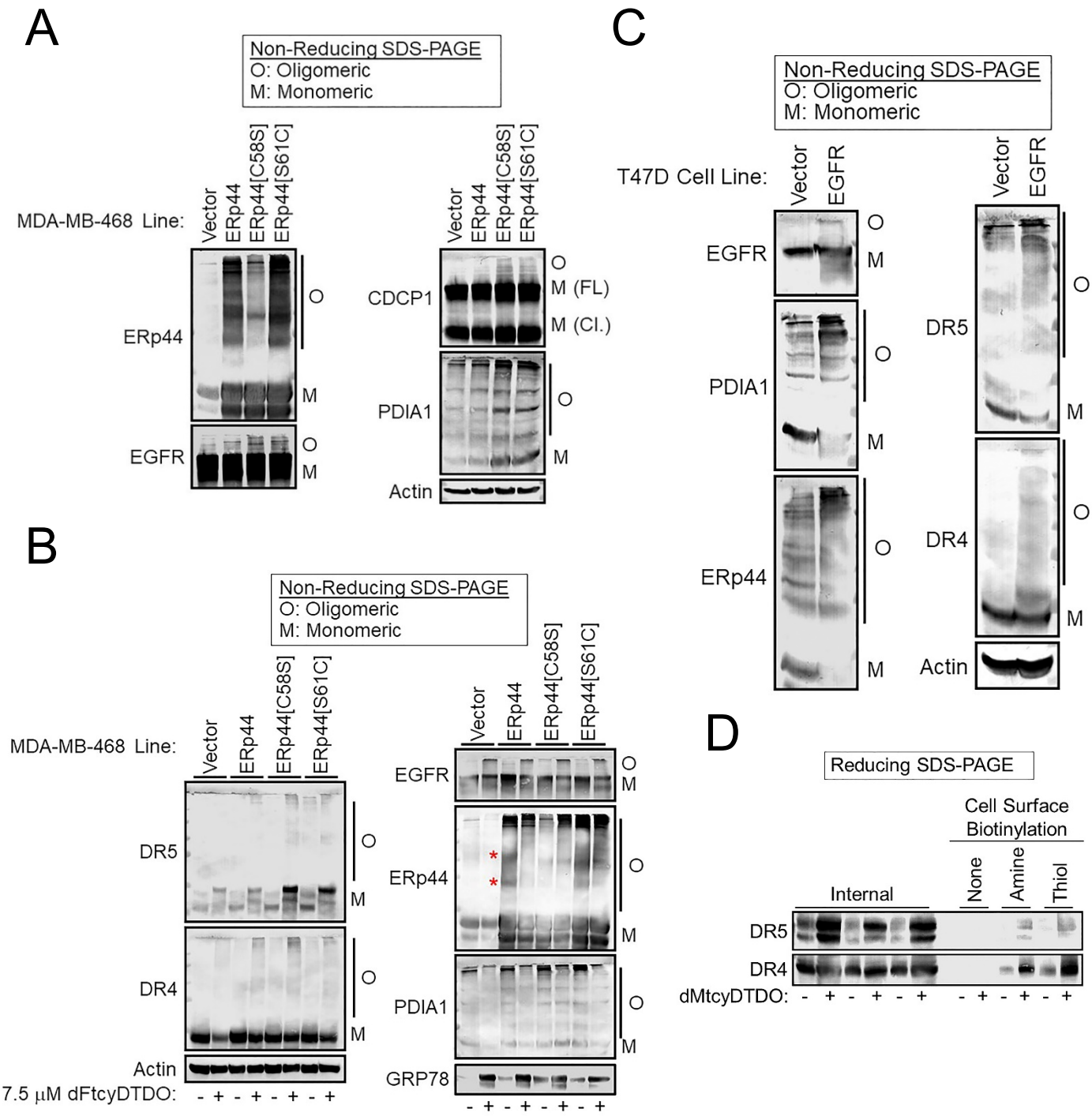

Fig. 5, Law et al.

A

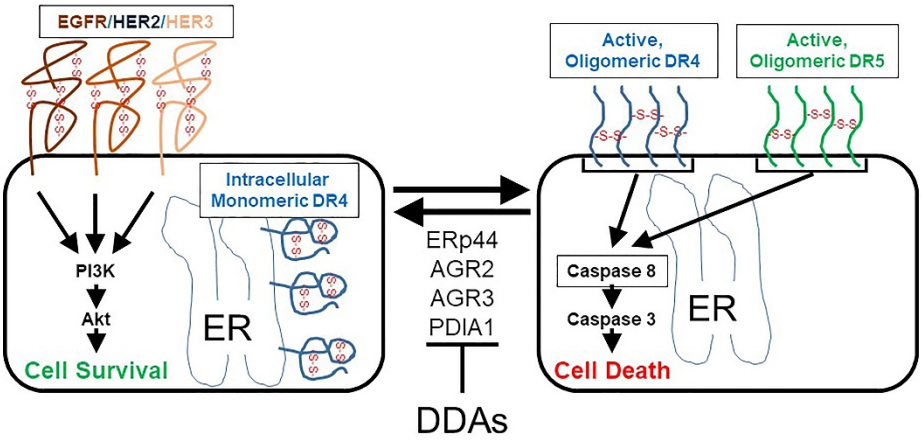

B

Substrate Trapping
Thioredoxin-like Repeats

AGR2: **C**PH**S**
AGR3: **C**QY**S**
ERp44: **C**RF**S**

C

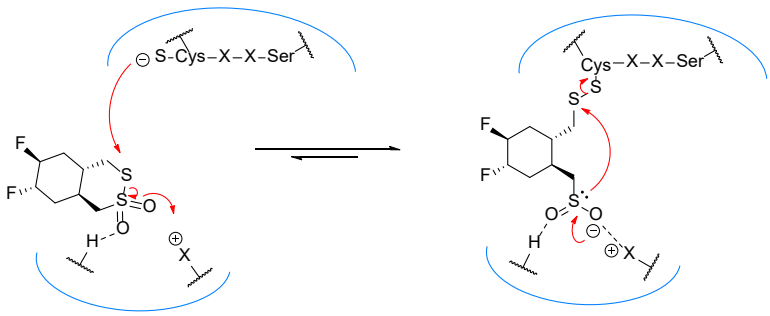

Fig. 6, Law et al.